Journal of Molecular Liquids 328 (2021) 115452

Contents lists available at ScienceDirect

Journal of Molecular Liquids

journal homepage: www.elsevier.com/locate/molliq

Interactions of natural deep eutectic solvents (NADES) with artificial and natural membranes

Helene Liepelt Nystedt *, Krister Gjestvang Grønlien, Hanne Hjorth Tønnesen

Section for Pharmaceutics and Social Pharmacy, Department of Pharmacy, University of Oslo, P.O. Box 1068, Blindern, NO-0316 Oslo, Norway

ARTICLE INFO

Article history:
Received 11 November 2020
Received in revised form 13 January 2021
Accepted 19 January 2021
Available online 23 January 2021

Keywords:
Natural deep eutectic solvents (NADES)
Artificial membranes
Natural membranes
Permeability

ABSTRACT

Natural deep eutectic solvents (NADES) are a third type of liquids, apart from water and lipids. NADES show promise as drug carriers in dermal formulations or formulations for local administration in the oral cavity due to their low toxicity, tunability and biodegradability as well as their solubilizing and stabilizing properties. However, a thorough investigation of their effects in a biological system is needed. The present study aimed to investigate the physicochemical properties of six selected NADES and dilutions thereof. Further, the suitability of NADES as vehicles in topical preparations was evaluated through the application of liposome model membranes and ex vivo pig skin models. The effects of NADES on the membrane stability of egg-phosphatidylcholine (Egg-PC) liposomes and 1,2-dipalmitoyl-*sn*-glycero-3-phosphocholine 16:0 PC (DPPC) liposomes were investigated by physical stability studies, membrane permeability studies, calorimetric analysis and visual representation by transmission electron microscopy (TEM). The liposomes appeared in most cases physically stable for 24 h in NADES, although there were changes in size and morphology most likely related to increased osmolality. Some NADES were also able to disaggregate formed DPPC liposome aggregates. The ex vivo permeation studies indicated a slightly reduced permeability of chloramphenicol through the pig skin after NADES application, which most likely was caused by hydrogen bonding between the NADES and proteins in the skin based on FT-IR-results. Altogether, our findings suggest that NADES are promising drug carriers in new drug delivery systems for topical applications.

1. Introduction

Natural deep eutectic solvents (NADES; used as both singular and plural in the following) have gained much attention lately for their potential as green solvents, as well as for their unique physicochemical properties [1]. A eutectic mixture is a system that has a lower melting point than any of its individual constituents when mixed in a specific ratio [2]. The melting point depression for NADES is large, resulting in them being liquid at ambient temperatures [3]. The components are generally natural metabolites, such as organic acids, amino acids, sugars and other small hydrophilic molecules. In general, deep eutectic solvents are considered less toxic, inexpensive, environmental friendly, biodegradable and less volatile compared to conventional solvents, such as ionic liquids (ILs) and organic solvents [4].

Since their discovery in 2011 [5], NADES have presented a range of possibilities for novel drug delivery systems as they are easily tunable and thermally and chemically stable [6,7]. Previous studies have shown that NADES possess unique properties as solubilizers and stabilizers in pharmaceutical formulation [8–11]. The solubilizing properties may in part be explained by a high polarity of the solvents, but also the spatial arrangement of interacting groups and differences in H-bond donating and accepting properties have been proposed [10]. NADES containing organic acids have also been reported to exhibit antimicrobial effects, possibly due to the low pH [12,13].

A thorough characterization of NADES could lead to further developments of new drug formulations. Even though the components are mostly natural primary metabolites, and thereby often presumed to be non-toxic and biocompatible, their effects in a biological system must be understood before they can be applied. Although a few studies on the toxicological aspects of NADES have emerged, the specific molecular interaction with e.g., the cell membrane is still not elucidated [14,15]. NADES could be potential drug carriers in a dermal formulation or possibly in formulations for local administration in the oral cavity [6,16,17]. Due to their previously mentioned antimicrobial activity, they would be especially relevant as pharmaceutical vehicles in antimicrobial treatments i.e., of chronic topical infections. Previous reports on ILs and DES indicate biofilm removing and preventing properties, possibly by disruption of the H-bond network present in biopolymers [18,19]. A topical application of NADES would result in direct contact between the liquid and the cell surface, and a thorough investigation of cell-solvent-interactions is therefore needed.

* Corresponding author.
E-mail address: h.l.nystedt@farmasi.uio.no (H.L. Nystedt).

https://doi.org/10.1016/j.molliq.2021.115452

Liposomes are widely used as artificial biological membranes because their structure is similar to a cell membrane, and they are easy and inexpensive to prepare and modify [20]. In the present study, we applied two different liposomal models: egg-phosphatidylcholine (Egg-PC) and di-palmitoyl-phosphatidylcholine (DPPC) to evaluate the effects of NADES on lipid bilayer membranes.

A recently published study by our group found that a NADES was able to dissolve collagen, which is an important structural component of the skin [17]. As mentioned above, one of the potential applications of NADES is in the development of dermal formulations. It would therefore be of interest to investigate how NADES may affect skin permeation. Skin is composed of extracellular matrix (e.g., collagen) and the potential interactions of NADES with both the biological membranes and collagen can affect the permeation and retention of active drug molecules. In the current study, we used a Franz diffusion cell with porcine ear skin as a model system to explore this, as porcine skin is considered an adequate substitute for human skin [21].

2. Materials and methods

All experiments were performed at 25 °C unless otherwise stated.

2.1. Materials

The following chemicals were purchased: 1,2-dipalmitoyl-*sn*-glycero-3-phosphatidylcholine >99% (Avanti Polar Lipids, Inc., Alabaster, AL, USA); egg-phosphatidylcholine >99%, chloramphenicol, calcein, betaine and sucrose (Sigma-Aldrich Co. LLC, St. Louis, MO, USA); choline chloride (AppliChem GmbH, Darmstadt, Germany); citric acid monohydrate (for analysis) and maleic acid (Merck kGaA, Darmstadt, Germany); glyserolum 85 per centum (Apotekerproduksjon AS, Oslo, Norway): xylitol 99% (Alfa Aesar GmbH & Co KG, Karlsruhe, Germany). All other reagents were of analytical grade and purchased from standard sources. Pig ears (butchered the same day) were purchased in frozen condition from butcher Strøm-Larsen (Oslo, Norway) and immediately stored at −18 °C.

2.2. Preparation of NADES

Six NADES were prepared by the vacuum evaporation method [10]. In brief, the components, whose amounts and molar ratios are portrayed in Table 1, were dissolved in 50 ml Milli-Q water (MQ-water) at 50 °C in a round bottom flask. When fully dissolved, the water was evaporated at 45 °C for 20 min with a rotary evaporator (Hei-VAP Value Digital, Heidolph instruments GmbH & CO, Osterode am Harz, Germany) to form a viscous liquid. All dilutions of the NADES after preparation were performed in 5 mM phosphate buffer of pH 6.8 (PB)($Na_2HPO_4{\cdot}2\ H_2O$ and $NaH_2PO_4{\cdot}H_2O$) at least 3 h before use unless otherwise stated. Undiluted NADES were stored in closed polypropylene tubes and protected from light. The buffer pH was adjusted to 6.8 to reflect the pH of skin (pH ~5.5) and saliva (pH ~6.7), which is relevant for the proposed applications.

Table 1
The composition of the NADES investigated in this study. The individual components were mixed in 50 ml water prior to evaporation.

NADES	Molar ratio	Component 1	Mass (g)	Component 2	Mass (g)
Acidic					
CS	1:1	Citric acid	10.507	Sucrose	17.115
ChM	1:1	Choline chloride	6.981	Maleic acid	5.804
CX	1:1	Citric acid	10.507	Xylitol	7.608
Neutral					
ChG	1:1	Choline chloride	6.981	Glycerol	4.605
ChX	5:2	Choline chloride	17.453	Xylitol	7.608
BS	2:1	Betaine	11.720	Sucrose	17.115

2.2.1. Water content

The water content of each NADES when undiluted was determined by Karl Fischer titration using a coulometer (C20 Coulometric KF titrator, Mettler Toledo Inc., Schwerenbach, Switzerland).

2.2.2. Preparation of diluted NADES samples with similar viscosity (NADES dilution series 1 (D1))

Each NADES was diluted to a viscosity of 1.1 mPa·s at 25 °C based on viscosity measurements. NADES CS, ChM and ChX were therefore diluted 1:10, whereas NADES CX, ChG and BS were diluted 1:15.

2.2.3. Preparation of NADES samples with similar water content (NADES dilution series 2 (D2))

The amount of water needed to gain a total water content of 40 (± 5)% (*w*/w) was calculated and added, based on the measured water content of each NADES.

2.3. Physicochemical characterization of NADES

2.3.1. Viscosity

The viscosity of NADES after addition of 0–70% (*v*/v) PB, was measured using a Brookfield Viscometer DV2T (Middleboro, MA, USA) with spindles CPA-40Z (low viscosity samples <10 mPa·s; accuracy ± 0.1 mPa·s) and CPA-52Z (high viscosity >10 mPa·s; accuracy ± 3.1 mPa·s). All measurements were performed in triplicate with sample volume 0.5 ml and a 2 min single point measuring method.

2.3.2. pH

The pH of NADES D1 was measured with a FiveEasy pH-meter with an InLab Micro electrode (Mettler Toledo, Columbus, OH, USA).

2.3.3. Refractive index

The refractive index (RI) of both dilution series of NADES at room temperature was measured using a Refractometer Abbe (Carl Zeiss 26,799, Germany), with a precision of ±0.0001.

2.3.4. Osmolality measurements

The osmolality of the samples of NADES D1 was measured using a Semi-Micro Osmometer (K-7400, Knauer Wissenschaftliche Geräte GmbH, Berlin, Germany), detection interval 0–2000 mmol/kg, accuracy and precision of ≤1%.

2.4. Preparation of liposomes

Both egg-PC liposomes and DPPC liposomes were produced by the thin-lipid film hydration method [22], followed by extrusion using a mini-extruder from Avanti Polar Lipids (Alabaster, AL, USA). The lipids were dissolved in chloroform in a round-bottomed flask, then evaporated at 40 °C to a dry lipid film with a rotary evaporator (Büchi R-100 Rotavapor with B-100 Heating Bath, Flawil, Switzerland). Residual solvent was removed by vacuum evaporation overnight (ALPHA 2–4 LD plus, Martin Christ Gefriertrocknungsanlagen GmbH, Osterode am Harz, Germany). The hydration medium (5 mM phosphate buffer pH 6.8) was added, followed by agitation of the suspension for 2 h. Extrusion was performed by passing the liposomes 19 times through a double layer of 200 nm polyethersulfone membranes (VWR International, LLC, West Chester, PA, USA). The final lipid concentration was 6 mM. Hydration and extrusion were performed at room temperature for the egg-PC and above 50 °C for the DPPC liposomes. For the calcein-loaded liposomes, the hydration medium contained 0.12 mM calcein.

2.5. Characterization of liposomes in NADES

All experiments were performed in triplicate and at 25 °C for both types of liposomes in NADES D1 and D2.

2.5.1. Physical stability

The particle size of the liposomes incubated in NADES was measured by dynamic light scattering (DLS) using a zetasizer (Nanoseries ZS, Malvern Panalytical, Spectris plc, Egham, Surrey, United Kingdom). The zeta potential was measured by the same instrument using a dip cell and the electrophoretic light scattering (ELS) method (ZEN1002, Malvern Panalytical, Spectris plc, Egham, Surrey, United Kingdom). All samples were measured 0, 3 and 24 h after start of incubation. The viscosity and RI of each sample was included in the mathematical model used for calculation of the DLS results.

2.5.2. Liposome permeability

The membrane permeability of liposomes in NADES was investigated using calcein as a fluorescent probe, as described in a previous report [23].

Calcein fluorescence in the selected diluted NADES was investigated in order to establish the experimental conditions to be applied in the release studies with fluorescence detection. The ultraviolet-visible (UV–Vis) absorption spectra and steady state fluorescence spectra were recorded. The concentration of calcein was 1.2×10^{-6} M.

UV–Vis spectra were recorded by a spectrophotometer (UV-2401PC, Shimadzu, Kyoto Japan). Fluorescence measurements were performed on a Photon Technology International modular fluorescence system (London, Ontario, Canada) with Model 101 monochromator with f/4 0.2-m Czerny-Turner configuration. The instrument was equipped with a red-sensitive photomultiplier. The excitation source was a 75 W xenon lamp. The emission and excitation spectra were automatically corrected for both the lamp spectral radiance and the detector quantum efficiency by means of the acquisition software (FeliX32, PTI). The excitation and emission monochromator band passes were set at 2 nm for recording of emission spectra. The excitation wavelength was set at the calcein absorption maximum detected in the respective NADES.

The fluorescence of calcein over time ($t = 30$ min) was measured with a fluorescence plate reader (Fluoroskan microplate fluorometer, Thermo Fischer Scientific, Waltham, MA, USA). Excitation and emission wavelengths were set to 485 and 535 nm, respectively. The amount of calcein released after time t was calculated as the percentage of maximal fluorescence according to Eq. (1).

$$\mathrm{RF}\ (\%) = \frac{100\ (I_t - I_0)}{(I_{max} - I_0)} \quad (1)$$

where I_t is the measured fluorescence intensity at time t, I_0 is the initial residual fluorescence of the liposomes and I_{max} is fluorescence after lysing the liposomes with 2% Triton X-100 (max. control).

2.5.3. Calorimetric analysis

Calorimetric measurements were conducted on DPPC liposomes in the presence of NADES using a Nano differential scanning calorimeter (Nano DSC 602000, TA Instruments, New Castle, Delaware, USA). Samples were analyzed 3 h after addition of NADES. The samples were scanned from 20 to 60 °C with a heating rate of 1 °C/min and under pressure of 3 atm. The amount of lipid in each sample was approximately 0,5 mg. The results were analyzed using the NanoAnalyze software from TA instruments.

2.5.4. Transmission electron microscopy (TEM)

The effects of NADES on the two liposome models were visualized by TEM using negative staining of uranyl acetate. Liposome samples containing NADES CS, CX or BS (D1) and liposomes in PB at two concentrations (50 or 150 μM) were freshly prepared. 10 μl drops of the samples were added on parafilm, followed by a 10 min adherence on carbon coated and glow discharged 100 hex mesh grids. The grid was sequentially treated with Milli-Q water, uranyl acetate (1% *w/v* in water), Milli-Q water, and uranyl acetate (0.4% w/v in water)/methylcellulose (1.8% w/v in water) and then dried under light. The samples were examined using a JEOL 1400Plus Electron Microscope (JEOL Ltd., Tokyo, Japan) equipped with a Ruby camera at 120 kV.

2.6. Effect of NADES on pig skin ex vivo

2.6.1. Preparation of pig skin samples

Pig ears were stored at −18 °C and thawed overnight in the refrigerator (4 °C) before sample preparation. Skin samples from the inside of the ear with a thickness of 1.2–1.3 mm were prepared, cutting off excess fat and cartilage with a fileting knife. A sharp hollow piston with diameter 2.3 cm was used to punch out individual skin samples. The outward facing side of the samples was soaked in undiluted NADES for 30 min before rinsing with 50 ml 0.15 M phosphate buffered saline (PBS) pH 7.4. Untreated skin samples rinsed with 50 ml PBS were used as controls. The skin samples were visually inspected for defects prior to and after the experiment.

2.6.2. Ex vivo permeation studies

Chloramphenicol (CAM) was selected as a model drug for the permeation studies. The method for ex vivo permeability studies of CAM through pig skin was obtained from another source [24] and modified for this study. The skin samples were inserted in Franz diffusion cells (PermeGear, Inc., Hellertown, Pennsylvania, USA), and the donor chamber was filled with 1.0 ml 2.5 mg/ml CAM in PBS. The acceptor chamber contained 8.0 ml PBS. The diffusion area was 1.00 cm^2. The Franz cell system was maintained at a constant temperature of 32 °C, and the acceptor medium was stirred constantly at 500 rpm throughout the experiment. Sampling from the acceptor chamber was performed every hour between time points 2–8 h and at 24 h. The withdrawn sample volume (100 μl) was immediately replaced with 100 μl PBS in the acceptor chamber. The samples were analyzed by HPLC and the cumulative amount of CAM in the acceptor chamber was calculated. All experiments were performed in triplicate.

Sink conditions were maintained based on previously performed solubility studies of CAM in PBS (Unpublished results), keeping the total concentration of CAM in the acceptor medium at <10% of the saturation concentration.

2.6.3. Quantification of CAM

Quantification of chloramphenicol was performed by HPLC analysis on a LC-20AD liquid chromatograph with a SPD-M20A UV–visible detector (Shimadzu, Kyoto, Japan) under the following conditions: A reversed phase C18 pre-column and column (Nova-Pak® 3.9 μm × 150 mm column, Waters, Milford, MA, USA), mobile phase consisting of MQ-water, methanol and anhydrous acetic acid (55:45:0.1 *v*/v), flow rate 0.8 ml/min, total run time 10 min, detection wavelength 275 nm, and column temperature 30 °C. The expected retention time of CAM was 3.3 min. The limit of detection (LOD) was 3.57×10^{-8} M and the limit of quantification (LOQ) was 1.19×10^{-7} M.

2.6.4. Fourier transform infrared spectroscopy (FT-IR) analysis of NADES treated pig skin samples

FT-IR spectra of untreated and NADES treated pig ear skin were acquired using a Nicolet™ iS™ 5 FTIR Spectrometer (Thermo Fisher Scientific, Waltham, MA, USA) with an iD5 diamond ATR Accessory. The skin samples were prepared and treated with NADES as described in 2.6.1. Samples were placed directly with the treated side on the diamond crystal. For each sample, 16 scans from 4000 cm^{-1} to 550 cm^{-1} were collected in single beam mode with a spectral resolution of 4 cm^{-1}. The samples were run in triplicates, confirming uniform samples.

Background spectra were acquired recording the spectra for an empty diamond crystal. The smoothed representative spectra (moving average and Savitzky-Golay filters) are presented. Second derivation of the curves were performed with the GraphPad Software (GraphPad Prism version 8.3.0 for Windows, GraphPad Software, San Diego, California USA, www.graphpad.com) to enhance the resolution of bands in the spectra.

2.7. Statistical analysis

The experimental data was presented as mean ± standard deviation from at least three independent experiments. The statistical analysis was performed using multiple *t*-test ($P < 0.05$) in the GraphPad Prism software.

3. Results and discussion

Three acidic and three neutral NADES were studied in the present work. The selection of NADES was based on previous results obtained by our research group [10,11,25]. The six NADES were physically stable and could be made with adequate reproducibility and at low cost. The dilution factor for NADES dilution series 1 (D1) was chosen based on viscosity measurements to eliminate viscosity as a factor in the experiments, and bring it closer to that of water. Excessive dilution could, however, weaken the NADES network [4,26,27]. Therefore, a second dilution series (D2) containing less water was prepared, with a final water content of 40% ± 5 (*w*/w). This was done to ensure that the water content of the samples was kept below 50%, which has been proposed as the critical limit for H-bond-formation in some NADES [28].

3.1. Physicochemical characterization of NADES

3.1.1. Water content and viscosity

Water has been found to be part of the structure in NADES [29]. The water is tightly bound and cannot be easily removed by evaporation. Depending on the preparation method, the water content in the NADES could be variable. As the water content affects the properties of the solvent, it should be quantified.

The measured water content of the undiluted NADES is presented in Fig. 1 a. The ChM sample was found to have the lowest water content of 10.5 ± 0.2%, while BS had the highest content of 22.9 ± 0.3%. The water content appeared to be independent of type of NADES (i.e., neutral or acidic), although both NADES containing citric acid (CS and CX) had a relatively high water content. This could be related to the hygroscopic nature of citric acid (and in part sucrose) or it could be a specific property of the NADES network. There was apparently a relationship between the intrinsic water content and initial viscosity, i.e., the higher the water content in the freshly prepared NADES the higher viscosity. The only exception was ChG which showed the lowest initial viscosity at a medium level intrinsic water content. The intrinsic water content is greatly dependent on the preparation method. In this study all NADES were prepared by dissolving the components in water prior to evaporation. Other methods, based on heating and stirring of components without addition of water, have resulted in significantly lower water content [30]. The high viscosity of NADES is most likely caused by numerous intermolecular bonds in the solvent [1]. It is therefore possible that NADES with very high viscosity were better able to incorporate water in their structure during preparation due to high H-bonding capacity.

The generally high viscosity of most NADES could hamper their potential use as pharmaceutical vehicles [3]. The viscosity of the selected NADES with up to 70% (*v*/v) added water was measured (see Supplementary Table S1), although only the range 0–40% (v/v) is presented in Fig. 1 b. The initial viscosity varied, ranging from ≈ 100 mPa·s for ChG to >1400 mPa·s for CS. However, the viscosity of NADES, particularly with a high initial viscosity, decreased rapidly upon addition of small amounts of water (Fig. 1 b). After addition of only 5% water, the viscosity of CS was reduced by ~65%. Addition of >30–40% water lead to a viscosity close to that of water in all samples. These results are consistent with other studies, showing a decrease in viscosity when small portions of water are added [28,31]. The decrease in viscosity is thought to happen due to a weakening of the strong intermolecular bonds in the eutectic solvent upon dilution. Dai et al. (2015) discovered through NMR analysis that the intermolecular H-bonds disappeared completely in some NADES when the water content reached >50% (*w*/w). Therefore, it must be taken into account that the special properties of the NADES may be lost with excessive dilution. Other studies have, however, shown that even very diluted NADES (up to 1:200 dilution) displayed different properties (i.e. lower bacterial toxicity) than a solution containing similar concentrations of the NADES components [12,17]. This suggests that the eutectic network could be weakly retained even at high dilution.

The possibility of adjusting the viscosity of NADES with water could present options for tailoring a pharmaceutical formulation according to area of application and application method. A formulation to be applied topically or onto oral mucosa should ideally not have too low viscosity to be retained at the application site.

3.1.2. Refractive index (RI), pH and osmolality of diluted NADES

The physicochemical characteristics, i.e., refractive index, pH and osmolality of the investigated NADES are shown in Table 2. The pH and osmolality were only investigated for NADES D1 due to practical difficulties with NADES samples with low water content (high viscosity and too low freezing point).

Due to the presence of an acidic component, the apparent pH of CS, ChM and CX was in the acidic range with a pH between 1 and 2 as

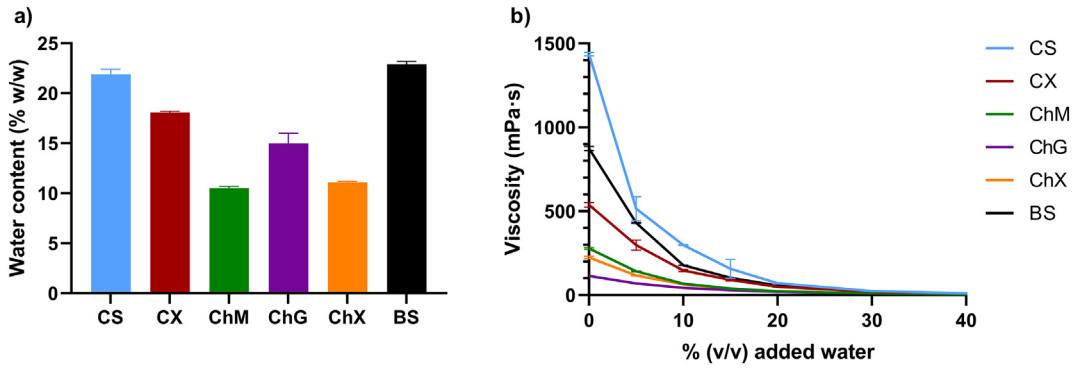

Fig. 1. Physical characteristics of prepared NADES. a) Water content (% *w*/w) of undiluted NADES ($n = 3$). b) Viscosity curves for the selected NADES as a function of added water (% *v*/v). Citric acid:sucrose (CS), citric acid: xylitol (CX), choline chloride: maleic acid (ChM), choline chloride: glycerol (ChG), choline chloride: xylitol (ChX) and betaine: sucrose (BS).

Table 2
Selected characteristics of undiluted NADES (D0) and NADES dilution series 1 and 2 (D1 and D2): water content, pH, refractive index (RI), viscosity and osmolality. PB = phosphate buffer.

NADES	D0		D1			D2	
	Water content (% w/w)	Viscosity (mPa·s)	pH (± 0.02)	RI	Osmolality (mOsm/kg)	RI	Viscosity (mPa·s)
Acidic							
CS	22	1437	1.87	1.346	606	1.425	17
ChM	10	278	1.07	1.349	1238	1.415	4.2
CX	18	538	1.85	1.342	363	1.415	11
Neutral							
ChG	15	114	6.49	1.344	853	1.417	5.1
ChX	12	224	6.63	1.349	1142	1.418	4.5
BS	23	874	6.78	1.337	330	1.424	12.9
PB			6.80	1.333	0.013		

expected. The remaining three NADES (ChG, ChX and BS) had a pH between 6 and 7, and were therefore considered as neutral.

The highest RI of 1.425 was measured for CS D2, while the lowest was for BS D1 at 1.337. The RI of the NADES samples was generally higher than the pure buffer sample, meaning the light was more refracted through the solvents. There was an increase in RI in D2 samples compared to D1 due to less water in D2. A previous study found that the RI values of NADES were linearly decreasing with increasing water content, which supports the present results [30]. The RI of the various NADES depends on the structure and bonds present in the solvent. A high RI value would in this case correspond to a tighter structure and more bonds between the molecules in the NADES network.

Osmolality is an important factor for liquid pharmaceutical formulations to be in direct contact with human cell membranes (e.g., wounds and oral mucosa). Blood and other extracellular fluids have an osmolality of ~280 mOsm/kg, corresponding to the osmolality of the intracellular fluids [32]. The measured osmolality of the NADES D1 samples ranged from 330 to 1238 mOsm/kg, with CX and BS in the low range (~350 mOsm/kg), CS and ChG in the middle (600–850 mOsm/kg) and ChM and ChX with the highest values (~ 1200 mOsm/kg). The NADES D1 samples had different water contents (see 3.1.1), and therefore different molar concentrations of components. Further, some of the constituents were able to dissociate, increasing the number of osmotic active components in solution. Three of the NADES contained choline chloride (ChM, ChX, ChG), which dissociates into two osmotic units independent of pH. All NADES containing choline chloride displayed high osmolality. The organic acids, maleic acid and citric acid, were weak and therefore not expected to give a significant contribution to the osmolality by dissociation. There was no obvious correlation between the acidity (e.g. acidic or neutral NADES) and osmolality.

3.2. Characterization of liposomes in NADES

3.2.1. Physical stability of liposomes

The particle size and zeta potential are important parameters when investigating the physical stability of a liposomal membrane. In the current study two liposomal models were used: egg-PC and DPPC.

Table 3 summarizes the measured zeta potential immediately after addition of NADES to the egg-PC and DPPC liposomes (t_0). Some of the samples were impossible to measure, most likely due to high conductivity or low mobility in the solvent. The zeta potential of egg-PC liposomes in the absence of NADES was slightly negative, which is consistent with other studies involving similar liposomes [33]. The zeta potential measurements showed a clear difference between liposomes incubated in the acidic NADES and the neutral ones. Except for liposomes in ChM, in which the liposome zeta potential was impossible to measure, the other two acidic NADES induced a positive shift in zeta potential for both egg-PC and DPPC liposomes. The positive shift was larger for the DPPC than the egg-PC liposomes, also when taking into account that the original DPPC liposomes were slightly less negative. For example, the zeta potential for DPPC liposomes in CX changed from 0.8 to 44.4 mV ($\Delta \approx 44$ mV), while the change was from - 4 to 20.2 mV ($\Delta \approx 24$ mV) for egg-PC in the same NADES. The D2 samples, which contained a higher NADES concentration, induced a larger shift than the D1 samples. The positive zeta potential could be related to the pH of the solution. Phosphatidylcholine, which is the main lipid in both egg-PC and DPPC, has a zwitterionic nature due to a quaternary amine group and a phosphate group in its hydrophilic head. A previous study has reported the intrinsic pKa value of the phosphate group in phosphatidylcholine to be 0.8, and it is 100% ionized when pH is >3 [34]. However, the apparent pH of the acidic NADES was measured to be between 1 and 2, where approximately 30–50% of the phosphatidylcholine molecules would have their phosphate groups protonated. This would lead to a net positive surface charge on the liposomes, as the quaternary amine group would remain positively charged [35].

The positive zeta potential could also be related to an excess of H^+-ions in the acidic solution. It has previously been proposed that the adsorption of H^+-ions to the surface of the liposomes could neutralize the negative charge of the phosphate groups [36]. A change from neutral to positive zeta potential as demonstrated in the current work could have implications for the application of these acidic NADES on human cell membranes if the same phenomenon occurs in vivo. Although pH effects on the lipid structure and dynamics have been little investigated in vivo, an acidic environment could affect lipid conformation, phase transition and membrane structure [37]. These effects could on the other hand be beneficial for antimicrobial treatment as they may destabilize a bacterial membrane and make them more vulnerable, i.e., in combination therapy. Another aspect to be considered is how a change in the cell membranes' zeta potential could induce interactions between a delivered drug and the membrane. The surface charge-modifying effect of NADES could also be exploited in a drug delivery system (DDS) based on polymer or lipid nanoparticles. Changing the zeta potential of the carrier could increase drug loading due to electrostatic interactions. This could be relevant when loading e.g. peptides or DNA/RNA into DDS [38].

The measured particle size of both liposome types incubated in NADES is presented in Fig. 2. The size of the reference egg-PC liposomes in buffer was measured to be 177.2 ± 10 nm and the polydispersity index (PDI) was 0.17 ± 0.02 (Figs. 2 a,b), indicating a reasonably narrow size distribution and low batch to batch variation. The reference DPPC liposomes showed a larger liposome size of 1010 ± 136 nm and a higher PDI of 0.64 ± 0.22 (Figs. 2 c, d). The zeta potential of these liposomes was virtually zero, leading to gradual aggregation after

Table 3
Zeta potential (mV ± SD) for egg-PC and DPPC liposomes mixed with NADES dilution series 1 and 2 (D1 and D2) and measured immediately.

NADES	Egg-PC		DPPC	
	D1	D2	D1	D2
Acidic				
CS	19.5 ± 0.8	21.2 ± 3.8	40.1 ± 2.4	26.2 ± 6.4
ChM	N.A.*	N.A.*	N.A.*	N.A.*
CX	20.2 ± 0.7	22.0 ± 1.9	44.4 ± 3.4	33.8 ± 3.1
Neutral				
ChG	−10.5 ± 2.9	N.A.*	−6.9 ± 1.2	N.A.*
ChX	−3.6 ± 1.3	N.A.*	N.A.*	N.A.*
BS	−4.1 ± 0.8	−22.8 ± 11.9	−1.9 ± 0.3	−8.3 ± 2.1
Without NADES	−4.0 ± 0.5		0.8 ± 1.0	

* N.A. = Not applicable.

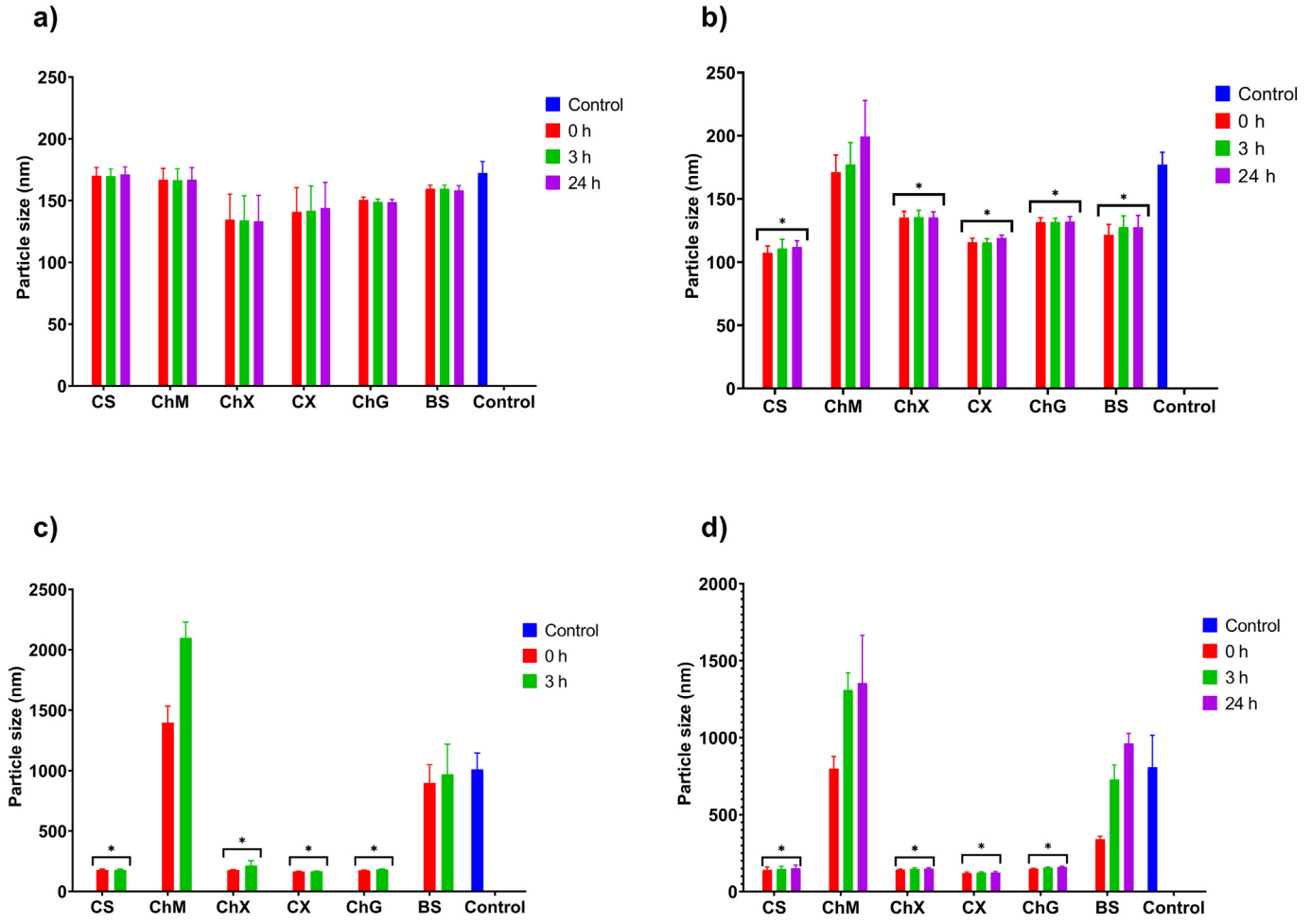

Fig. 2. Particle size of egg-PC and DPPC liposomes after incubation in NADES (0, 3 and 24 h). a) Egg-PC liposomes in NADES dilution series 1 (D1), b) Egg-PC liposomes in NADES dilution series 2 (D2), c) DPPC liposomes in NADES D1, d) DPPC liposomes in NADES D2. * Significant size reduction compared to control ($P < 0.05$).

preparation. The size of the egg-PC liposomes in NADES D1 was not significantly different from the reference, although some samples (ChX, CX, ChG and BS) seemed to induce a slight size reduction compared to the reference (Fig. 2 a). The size of the liposomes in the NADES D2 samples was, however, generally reduced compared to the reference and was significant in the case of CS, ChX, CX, ChG and BS (Fig. 2 b). The size of the egg-PC liposomes remained unchanged after the initial size reduction for all samples except ChM D2. The reason for the reduction is not completely clear, but could possibly be related to changes in osmolality. The components of NADES form a strong network, as well as being hydrophilic and often ionic, and hence the membrane penetration of the NADES components would most likely be limited, resulting in hypertonicity as confirmed by the osmolality data (Table 2). The core of the egg-PC and DPPC liposomes applied in this experiment contained a very weak (5 mM) phosphate buffer with osmolality close to zero. Thus, the osmolality of all the NADES samples was considerably higher than the osmolality inside the liposomes. The relationship between the osmolality of other solvents and liposome size has been thoroughly investigated by Sabin et al. (2006) [39]. They concluded that a concentration gradient over the semi-permeable liposomal membrane lead to an outgoing flux of water to compensate for the hypertonic conditions, followed by shrinking of the liposome. This is consistent with the well-known fact that a hypertonic solution will temporarily shrink red blood cells when given intravenously.

Another issue to consider is the limitation of the DLS-method when comparing samples in different solvents. Calculation of liposome size is based on the fluctuation of light intensity due to Brownian motion of the particles in solution. Even when adjusting for differences in viscosity and RI there may be other properties of the solvent affecting particle movement, e.g., the hydrogen bonding structure of the NADES network [28].

It was difficult to measure the real particle size of the reference DPPC liposomes due to aggregation and large variations between parallels depending on time of measurement after preparation. The reported size in Figs. 2 c, d was most likely affected by aggregates and thus much larger than the actual liposome size. It was, however, interesting to observe that some of the NADES broke up the aggregates and stabilized the liposome size immediately when added to the dispersion. Four of the NADES posessed aggregate breaking properties: CS, ChG, ChX and CX (Figs. 2 c, d). The disaggregation remained constant over 24 h for the D2 samples (Fig. 2 d). The D1 samples were only tested at 0 and 3 h for practical reasons, but the disaggregation was maintained over this time interval. The aggregate breaking effect of NADES did not seem to be related to pH. It is well-known that the zeta potential is an important factor in particle aggregation. According to the DLVO-theory, particles aggregate when the electrostatic repulsion is too weak to create an efficient energy barrier against the combined kinetic energy and van der Waals attraction between the particles [40]. The further apart the zeta potential is from zero, the stronger electrostatic repulsion is experienced between the particles. A high zeta potential (independent of the charge) will thereby prevent the particles from aggregating, creating a physically stable dispersion. The results of the aggregate breaking

NADES showed that both the CS and CX samples (D1 and D2) resulted in a strongly positive zeta potential (26–44 mV) of the DPPC liposomes (Table 3). ChG also altered the zeta potential, albeit in a negative direction, to approximately −7 mV. The zeta potential of the liposomes in the last aggregate breaking NADES (ChX) could not be measured. It is therefore unclear if this zeta potential was changed. The zeta potential of the liposomes in the non-aggregate breaking NADES could only be measured for the BS samples. It was close to zero (~ −2 mV) for the BS D1 sample but slightly more negative at −8 mV for BS D2. The latter value was quite similar to the aggregate breaking ChG D1 sample. This indicates that the zeta potential was not the only factor affecting aggregation of the liposomes. However, the disaggregation appeared mostly to be related to the change in zeta potential.

3.2.2. Liposome permeability

The study of liposome permeability is a frequently used method to investigate membrane stability. Calcein was loaded into the liposomes to serve as a fluorescent probe. It is expected that calcein enveloped inside a liposome will self-quench at high concentrations leading to an increase in fluorescence intensity upon release [41]. The calcein release over time from liposomes incubated in NADES D1 and D2 is shown in Fig. 3. The results for NADES BS were not included because a precipitate formed when calcein was added. The calcein release from both egg-PC and DPPC liposomes increased slightly over time in the NADES samples compared to the reference, with the exception of CX D1 and D2. CX and BS D1 had lower osmolality than the other measured samples (Table 2), thus possibly inducing less outgoing flux from the liposomes. However,

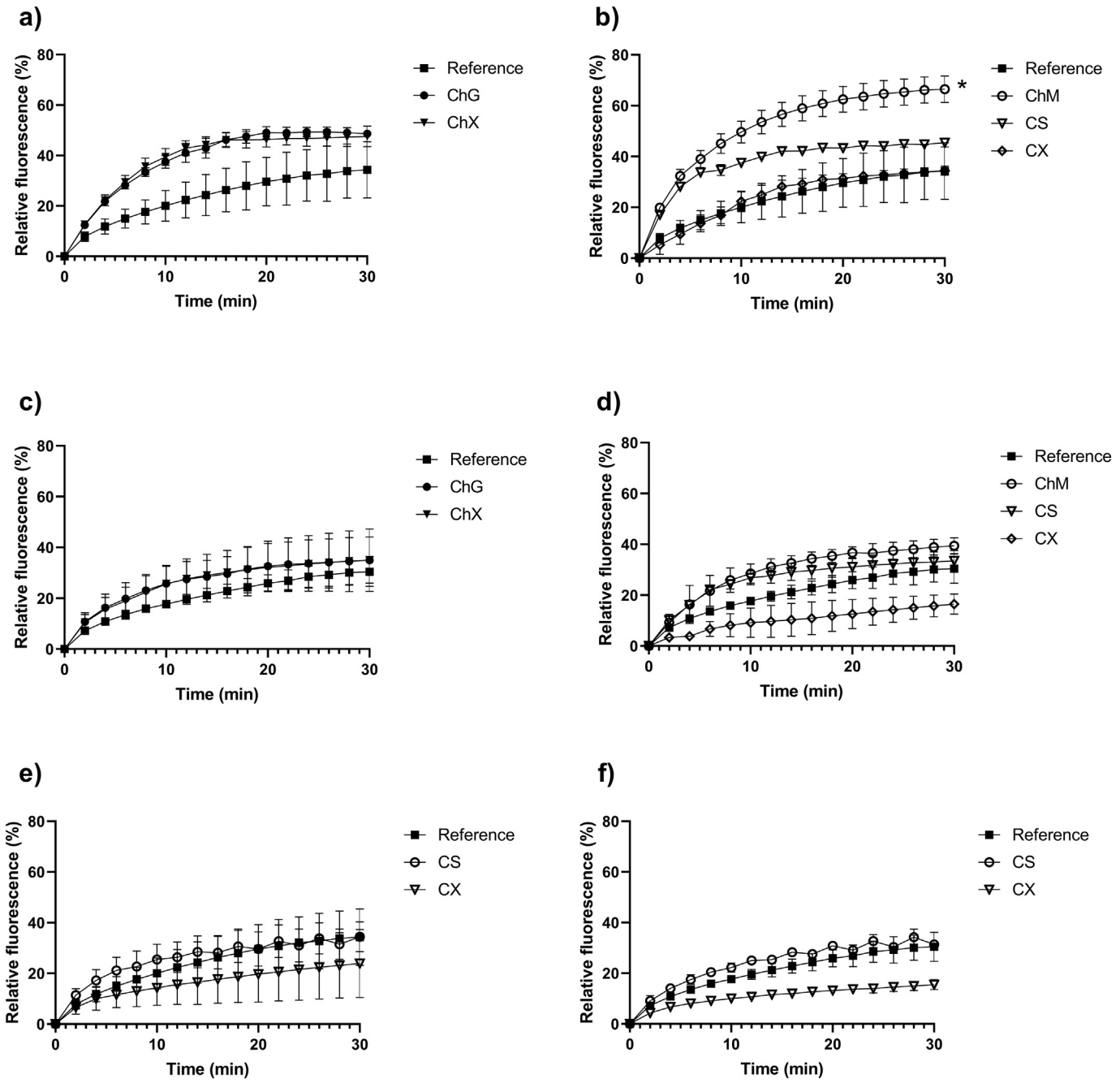

Fig. 3. Release profile for calcein from egg-PC and DPPC liposomes incubated in NADES dilution 1 (D1) and dilution 2 (D2). a) Egg-PC liposomes in neutral NADES D1, b) Egg-PC liposomes in acidic NADES D1, c) DPPC liposomes in neutral NADES D1, d) DPPC liposomes in acidic NADES D1, e) Egg-PC liposomes in selected NADES D2, f) DPPC liposomes in selected NADES D2. *Significant difference compared to reference ($P < 0.05$).

the calcein release in the BS D1 and D2 samples was higher than the CX samples. The low release of calcein in the CX samples indicates that this NADES had a slight membrane stabilizing effect on these liposomes. The calcein release from egg-PC liposomes in acidic NADES varied more compared to the neutral solvents. The difference between the lowest and highest total release of the D1 samples ended up being ~37% (CX = 37.8% vs. CS = 75.3%). The egg-PC liposomes in neutral NADES were quite similar in terms of total calcein release, with a difference of just ~13% between the highest and lowest release. The results from the D2 samples of CS, CX and BS are shown in Figs. 3 e, f. The release of calcein was significantly lower in the CS and CX samples compared to the D1 samples with similar NADES. The liposome size measurements of the samples showed a significant reduction of particle size in the CS and CX D2 samples compared to D1. A reduction in particle size indicated that the phospholipid membrane would be tighter, thus reducing the permeability. Further, the diffusion area (i.e. surface of the liposome) would be reduced, which could account for the lower calcein release rate.

Temperature is an important factor for diffusion through liposome membranes because it determines the physical condition of the lipids. The gel-to-liquid transition temperature (T_m) of DPPC is approximately 41 °C. The liposome permeability experiments were performed at 25 °C, meaning that the DPPC lipids were in the gel-phase. Liposomes in the gel-phase have previously been reported to exhibit reduced membrane permeability [42]. The T_m of egg-PC on the other hand is around −15 °C, meaning that these lipids were in the liquid-phase during the experiment. The egg-PC liposomes are expected to be more similar to a biological membrane than DPPC, due to the content of a combination of several different phosphatidylcholines. However, the total calcein release in the reference samples of egg-PC and DPPC liposomes was only slightly different (~4%), with a calcein release of 34% and 30% for egg-PC and DPPC liposomes, respectively (Figs. 3 a, c). Aggregation is another factor to be considered regarding the results for the DPPC liposomes. The calcein release from aggregated liposomes should be reduced due to a reduction in total surface area while aggregate breaking NADES could be expected to facilitate release. A certain trend can be seen where three of the aggregate breaking NADES (CS, ChG and ChX) gave very similar and somewhat higher release of calcein than the others (Fig. 3). The difference was, however, not significant.

3.2.3. Calorimetric analysis

Calorimetric measurements and thermograms can give much information about stability of and interactions with the liposomal membrane. Only the DPPC liposomes could be investigated by this method because the phase transition temperature (T_m) of egg-PC liposomes was outside the detection range of the instrument. The results showed that the pretransition present in the thermogram of the DPPC liposomes in buffer disappeared in the presence of acidic NADES (ChM, CS and CX, Fig. 4). In the case of the acidic NADES (ChM, CS and CX) no other peaks than the main transition peak could be detected. The thermograms of liposomes in neutral NADES (ChG, ChX and BS) on the other hand, showed a pretransition peak in their thermograms, although the shape and temperature (T) of the peak varied between the samples. The pretransition peak of DPPC liposomes is linked to the so-called "ripple phase", which occurs in the transition between the gel and liquid phases [43].

Crowe and Crowe in 1991 [44] investigated the effect of different sugars on the thermotropic phase transition of DPPC liposomes. According to their results the pretransition is only present for multi lamellar vesicles (MLV) DPPC liposomes, and not for unilamellar liposomes. The liposomes used in the current study were extruded and were therefore considered unilamellar. However, the extruded liposomes aggregated quickly, which might have led to thermotropic properties similar to that of MLVs [45]. In that case, the pretransition peak in the thermograms of DPPC in the presence of the aggregate breaking NADES should be absent. This appears to be true for the liposomes in CS and CX, which seem to only exhibit the main transition peak (Table 4). The pretransition peak found in the thermograms of liposomes in aggregate-breaking ChX and ChG showed a higher T_m than the pretransition peak of the liposomes in buffer, which might be related to a different thermal event than the ripple phase. If the hypothesis regarding thermotropic similarities between aggregated liposomes and MLVs was correct, the pretransition peaks should be present in the thermograms of the liposomes in the non-aggregate breaking NADES (i. e. ChM and BS). However, this was not the case, which indicated that the disappearance of the pretransition was most likely not caused by the break-up of the liposome aggregates. Thus, there seems to be other properties of the NADES leading to a disruption of the membrane, but it is unclear what this means for the physical stability of the liposomes.

Crowe et al. [44] have reported that a high concentration of different sugars (sucrose, trehalose and fructose) induced a second peak with lower T_m, leading to a shoulder-like shape in the thermogram, as seen for ChG, ChX and BS (Fig. 4). All these three NADES contain sugar-like compounds that could explain this effect. This might suggest that some of the sugars interacts with the lipid.

The T_m of the main transition was generally slightly higher (0.7–2.2 °C) for all DPPC samples containing NADES, compared to the pure DPPC liposomes (Table 4). The increase appeared virtually constant with the exception of ChM. According to Crowe and Crowe

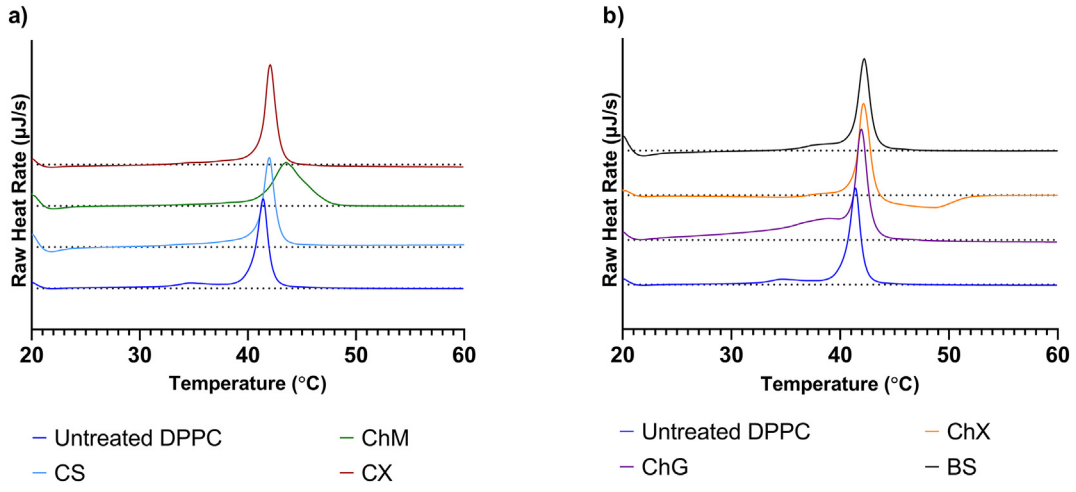

Fig. 4. Thermogram of DPPC liposomes incubated for 3 h in NADES dilution 1 (D1). a) acidic NADES, b) neutral NADES.

Table 4
Calorimetric results for DPPC liposomes incubated for 3 h in NADES dilution series 1 (D1).

	T_m (°C)	Δ T_m	T_m of pretransition	ΔH_{total} (kJ/mol)	ΔS (kJ / (mol·K))
DPPC	41.3		32.0	29.3	0.093
Acidic NADES					
CS	42.0	+ 0.7	-*	28.4	0.090
ChM	43.5	+ 2.2	-*	30.9	0.097
CX	42.1	+ 0.8	-*	32.7	0.104
Neutral NADES					
ChG	42.0	+ 0.7	39.0	35.2	0.112
ChX	42.2	+ 0.9	38.4	18.3	0.058
BS	42.2	+ 0.9	37.9	28.6	0.091

* No pretransition peak was detected.

(1991) the increase in T_m might be caused by osmolar dehydration due to a created concentration gradient across the membrane [44]. This effect was also reported in another study [46]. Although a higher T_m could mean increased membrane stability, the results are inconclusive. There was apparently no correlation between the changes in T_m and the calcein release profiles (Fig. 3) or the osmolality of the solvent (Table 2).

The thermogram of DPPC in the presence of ChM differed from the other thermograms both in terms of shape and an increase in T_m (Fig. 4, Table 4). The higher T_m could mean increased thermal stability. However, the completely different shape of the phase transition peak could indicate disruptions of the liposome membrane. This was further confirmed by the DLS results, where the liposome size was gradually increasing in the ChM D2 sample (Figs. 2 b, d), as well as the high calcein release from egg-PC liposomes in ChM D1 (Fig. 3 b).

3.2.4. TEM imaging of liposomes in NADES

TEM images of egg-PC and DPPC liposomes in three selected NADES D1 samples (CS, CX and BS) are shown in Fig. 5. The lipid concentration had to be adjusted individually for each sample due to variable adherence of liposomes to the grid surface. A carbon coated and glow discharged grid resulted in better adherence than formvar coating and was therefore used. The largest liposomes appeared to be in the same size range as the DLS measurements indicated (~170–200 nm diameter, Fig. 2), although some appeared to be larger. The negative staining technique is known to "flatten" the liposomes, thereby increasing their perceived size [47]. The size distribution of the liposomes was wider in the TEM images than the DLS measurements indicated. This was mostly due to an apparent second population of smaller size (~50–100 nm diameter). However, it is unclear if the difference in size distribution is related to imprecision in the DLS method or occurrences in sample preparation for TEM.

The shape of the egg-PC liposomes was spherical, except for the CX sample where the liposomes were more oval shaped. The surface morphology did, however, vary between the samples. The egg-PC liposomes in CS had a peculiar "cup-shape" that was less expressed in the other samples. Previously in this work it was discussed how increased osmolality could decrease the liposome size. The reported osmolality of CS D1 was twice as high as CX D1 and BS D1 (Table 2). This further emphasized that the observed shrinkage of the liposomes might be caused by hypertonicity. It was not investigated whether this effect was reversible after further dilution of the sample.

The DPPC liposomes appeared more faceted compared to the egg-PC liposomes, which was expected because the DPPC lipids are more rigid in the gel-phase [48]. The results obtained from DLS measurements showing aggregation of the DPPC liposomes were further confirmed by the TEM imaging. No aggregation was observed in the CX and CS samples. This was consistent with the DLS measurements and emphasized that addition of these NADES induced disaggregation of the liposomes.

3.3. Effect of NADES on skin

3.3.1. Ex vivo permeation

The ex vivo permeability study was performed by investigating the diffusion rate of chloramphenicol (CAM) through porcine ear skin pretreated with NADES. Chloramphenicol was chosen as the model drug

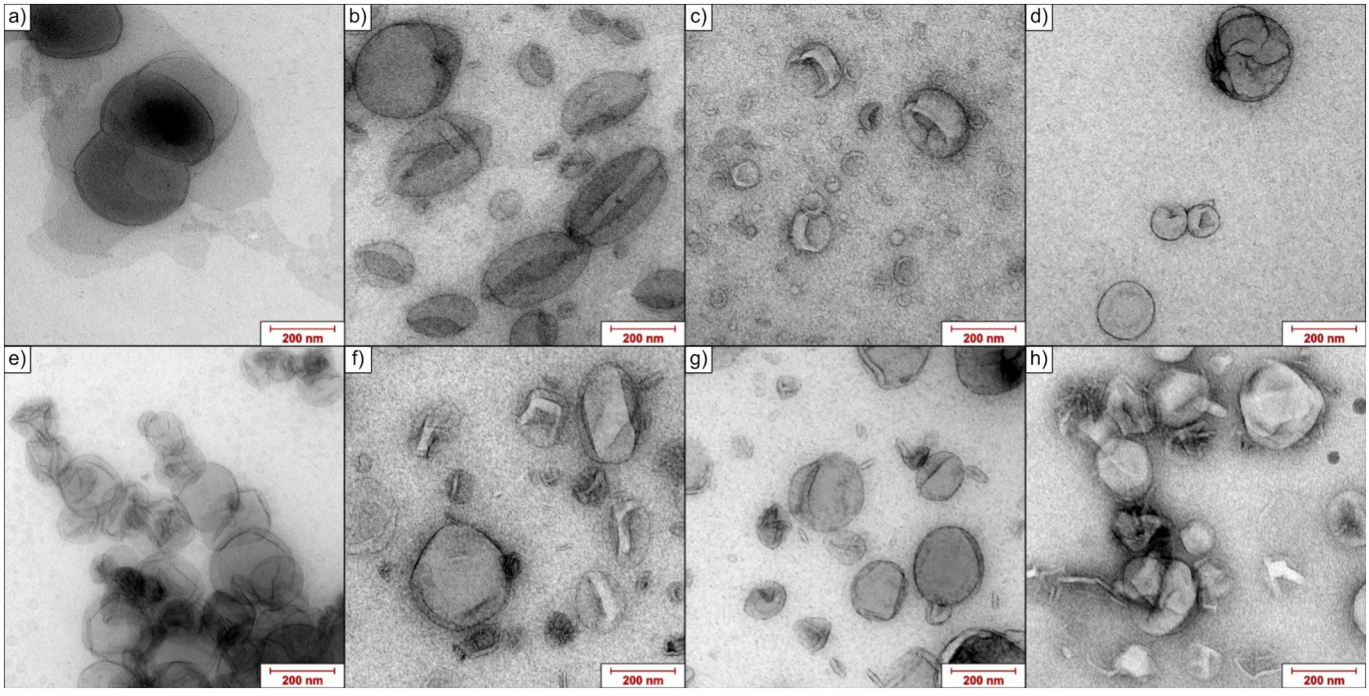

Fig. 5. Transmission electron microscope images of egg-PC and DPPC liposomes in NADES dilution series 1 (D1). a) Egg-PC (50 μM) in buffer, b) egg-PC (150 μM) in CX, c) egg-PC (50 μM) in CS, d) egg-PC (150 μM) in BS, e) DPPC (150 μM) in buffer, f) DPPC (150 μM) in CX, g) DPPC (50 μM) in CS, h) DPPC (150 μM) in BS. Scale bars = 200 nm.

because it represents an interesting candidate for novel dermal formulations, as discussed by Ingebrigtsen et al. [24]. Previous work in our lab has shown that certain NADES are able to dissolve collagen [17], and this could be expected to contribute to an improved permeability through skin. However, according to the results, the permeability appeared to be reduced after treatment with NADES. The permeability was significantly lower through all of the NADES-treated samples after 8 h compared to the reference (Fig. 6 b). The effect was, however, less pronounced at 24 h. There was no significant difference between the individual NADES at any time point. It was visually observed that the skin seemed to change appearance by becoming "stiffer" and curled after being soaked in NADES (Fig. 6 a). These changes might be the result of the collagen-dissolving effect of NADES, through a destruction of the connective tissue. However, this does not explain why the diffusion of CAM was reduced. Previously in the discussion a possible osmotic dehydration effect of NADES on the liposomal membrane has been proposed. A similar effect might also be valid for porcine skin cells, especially since the NADES were applied undiluted. Dehydration may contribute to reduced skin permeability. This is supported by studies showing that permeability is better through well hydrated skin [49,50].

Depending on the clinical purpose, enhanced skin permeation could be a desired or undesired effect of NADES. For local treatment of skin infections with for example CAM or another antimicrobial agent, pronounced skin penetration of the drug is unwanted due to the risk of systemic effects. However, if the permeation is too restricted, the drug might not reach into all the infected tissue. NADES could also be of interest in formulations for oral application. The effects of NADES on penetration through the mucosa in the oral cavity would not be relatable to the effects on skin, as the barriers are quite different. Further investigation into the effect of NADES on skin and oral mucosa is warranted to better understand their potential in a clinical perspective. Another issue to address is whether the eutectic will be administered in an undiluted or diluted form at the application site. In the ex vivo permeability study NADES was applied undiluted, although most of the experiments in this paper have been conducted on diluted NADES to lower viscosity for practical reasons. However, for application on surfaces like skin and oral mucosa, a certain viscosity is needed for sufficient retention of the formulation at the administration site. Further, the NADES network could be weakened by excessive dilution, as discussed in 3.1.1. Thus, the dilution ratios of NADES used in this work are not necessarily optimal in formulations for clinical application.

3.3.2. Structural changes in skin due to NADES treatment

Skin consists of a relatively small number of major constituents, including collagen, keratin, certain carbohydrates and lipids, which makes FT-IR and other techniques visualizing molecular structure suitable for studying structural changes in the skin [51]. A previous study on the transdermal delivery of APIs by application of deep eutectics as

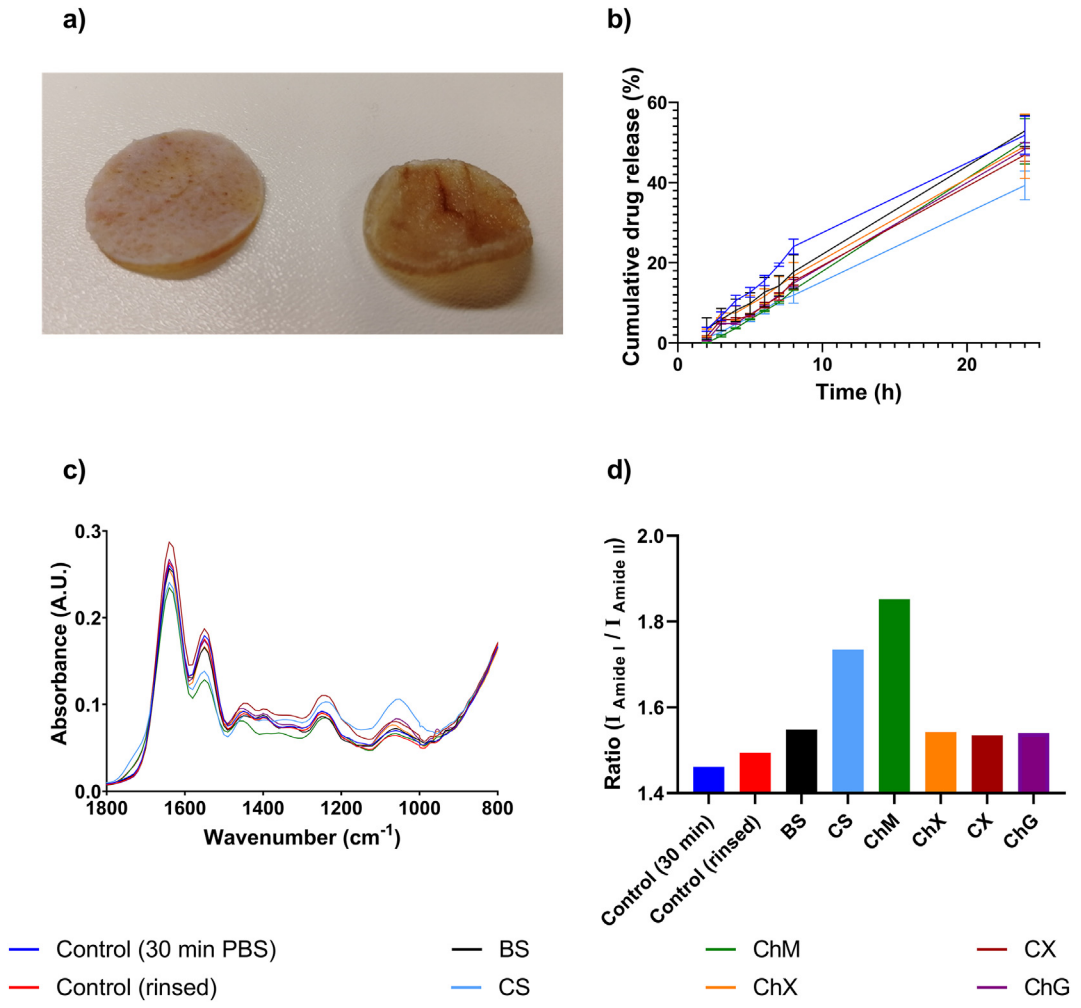

Fig. 6. Characteristics of pig skin treated with undiluted NADES for 30 min, then rinsed with 50 ml PBS. Skin samples had a diameter of 2.3 cm. a) Image of untreated (left) and treated pig skin (right). b) Permeability of chloramphenicol (CAM) over 24 h through pig skin after NADES treatment. Significantly lower permeability at 8 h through samples treated with CS, CX, ChG and ChM ($P < 0.05$). c) FT-IR spectra of pig skin after NADES treatment. d) Ratio of intensity (I) between amide I and amide II based on FT-IR results of pig skin after NADES treatment.

penetration enhancers have focused on the lipid content of the stratum corneum (SC). In that study, the SC was separated from dermis by soaking full thickness skin in heated water baths and trypsin digesting of the epidermis from the SC [52]. The mentioned study found that the eutectic solvent acted as a lipid extractor to improve the permeability of drugs [52]. Our results did not express distinct bands in the area related to lipids and their CH_2 symmetric and asymmetric stretching bands between 2800 and 3000 cm^{-1}, most likely due to a difference in preparation of the skin samples and pretreatment methods. However, when applying the second derivative to the spectra, it was possible to determine some of the band positions, including the symmetrical and asymmetrical CH_2 stretching (Fig. S1 a, Supplementary material). Bands related to proteins and lipids <1800 cm^{-1} were clearly present (Fig. 6 c). The untreated pig skin samples exhibited distinct vibrational bands corresponding to C=O stretch of amide I (1641 cm^{-1}), N-H bend and C-N stretch of amide II (1550 cm^{-1}), bending of CH_2 ($\delta(CH_2)$) and asymmetrical bending of CH_3 ($\delta_{as}(CH_3)$) of proteins and lipids (1450 cm^{-1}), C=O stretch and CH_3 bending of COO^- for proteins and lipids (1400 cm^{-1}), $\delta(CH_2)$-wagging (1328 cm^{-1}), C-N stretch, N-H bend and CH_3-C stretch of amide III (1240 cm^{-1}) and CC stretching and $\delta(CH_2)$ (1180 cm^{-1}). A broad band at 1061 cm^{-1} corresponding to either phospholipids or carbohydrates was also present. The bands were confirmed by the second derivative of the spectra (Fig. S1 b, Supplementary material). In this study, we focused on the amide I, amide II and $\delta(CH_2)$ bands, typical for skin samples [53,54]. Since the pig skin samples were rinsed with 50 ml PBS prior to the FT-IR scan, the NADES itself was considered to give little to no contribution to the spectra.

There were no differences in the positioning of the amide I or II bands in the NADES treated samples compared to the controls. However, the intensity of the bands for the pig skins treated with acidic NADES were different compared to the controls. The intensity of the amide I band may be an indication of water absorption by the skin, and the signal will increase upon water absorption. The amide II band is, however, not influenced by water absorption, which makes the ratio between the two amides an indication of the water absorption [55–57]. The ratio between amide I and II was remarkably higher for pig skin samples treated with ChM and CS (Fig. 6 d). This correlates with the low average permeability of CAM (although not significantly lower than untreated samples) through the skin up to 6–8 h. However, an increase in water content (often caused by occlusion of skin) is associated with increased permeability, which indicates that the higher ratio for ChM and CS may be caused by hydrogen bonding between the NADES and the amide rather than a high water content [58]. Amide *I* and II are recognized as sensitive markers for protein secondary structure. However, amide II is less affected by side-chain vibrations and more difficult to correlate to the secondary structure, and was therefore not discussed further [59]. According to the literature, an amide I band located at 1640 cm^{-1} corresponds to either a β-sheet or a disordered, random coil, secondary protein structure [53,59]. The pig skin samples were frozen and thawed, which can influence the protein structure.

Three of the NADES (CX, CS and ChM, all being highly acidic) expressed a tail on the amide I band (around 1740 cm^{-1}), which could correspond to the C=O stretch of phospholipids, esters and glycerides, but could also be the C=O stretching signal of the acid component [53,60,61]. The latter was most plausible, as the control did not express this band. This will as well explain a hydrogen bonding between the NADES and amide I, with the NADES being a hydrogen bond acceptor and the amide acting as a hydrogen bond donor [58]. CX and ChM expressed differences in the $\delta(CH_2)$ and $\delta_{as}(CH_3)$ bands (overlapping bands, which may be caused by interactions between closely packed lipid chains), with CX expressing higher intensity bands and a red shift, and ChM expressing lower intensity bands, with a blue shift [54,62]. NADES treated samples generally expressed a shift to longer wavenumbers (i.e., blue shift) for these bands, except CX and CS, which may indicate changes in the lipid structure. The intensity of symmetrical and asymmetrical CH_2 stretching (second derivative) for ChM indicated a lipid extracting effect of this NADES.

It was difficult to conclude whether the structural changes in the skin had an impact on the permeability from the inconsistent results on CAM diffusion through pig skin after NADES treatment. However, the apparent lower diffusion rate after 6–8 h may be caused by hydrogen bonding between the NADES and the proteins in the pig skin, decreasing the permeability.

4. Conclusions

The application of NADES in drug formulation is still in the initial stage and requires thorough investigation to ensure efficacy and safety. An important step on the way is characterization of the physicochemical properties of these solvents and their possible interactions with membranes. The components and structure of NADES play an important role in their properties and offer a wide range of opportunities for modifications and tailoring of these solvents. The stability studies showed that the liposomes in most cases were physically stable in NADES throughout a 24-h period, and in some cases were further stabilized by the solvent as demonstrated by an increased melting point of the lipid. A reduced liposome size and "folding" of the liposomes were observed when incubated in the NADES D2 samples, most likely caused by the high osmolality of the solvent. The ex vivo permeation studies indicated a slightly reduced permeability of CAM through skin after NADES application, which was proposed to be caused by hydrogen bonding between the NADES and proteins in the pig skin based on FT-IR-results. However, the results were inconclusive. NADES show a great promise as potential new pharmaceutical vehicles for topical administration, and further biological characterization would be an important step toward their use in drug formulations.

Funding

This research did not receive any specific grant from funding agencies in the public, commercial, or not-for-profit sectors.

Declaration of Competing Interest

The authors declare that they have no conflict of interest.

Acknowledgements

The authors are grateful to Dr. Raj Kumar Thapa and Prof. Gro Smistad, Department of Pharmacy, University of Oslo, and Ulrike Böcker, Nofima AS for valuable discussions. The authors are also grateful to Ivar Grove, Bente Amalie Breiby and Tove Larsen, Department of Pharmacy, University of Oslo and Jens Wohlmann, Department of Biosciences, University of Oslo for technical support.

Appendix A. Supplementary data

Supplementary data to this article can be found online at https://doi.org/10.1016/j.molliq.2021.115452.

References

[1] Y. Dai, J. van Spronsen, G.-J. Witkamp, R. Verpoorte, Y.H. Choi, Anal. Chim. Acta 766 (2013) 61.
[2] Y. Marcus, Springer Nature Switzerland AG, Cham, Switzerland, 2019, 205.
[3] L.K. Savi, D. Carpiné, N. Waszczynskyj, R.H. Ribani, C.W.I. Haminiuk, Fluid Phase Equilib. 488 (2019) 40.
[4] Y. Liu, J.B. Friesen, J.B. McAlpine, D.C. Lankin, S.-N. Chen, G.F. Pauli, J. Nat. Prod. 81 (2018) 679.
[5] Y.H. Choi, J. van Spronsen, Y. Dai, M. Verberne, F. Hollmann, I.W.C.E. Arends, G.-J. Witkamp, R. Verpoorte, Plant Physiol. 156 (2011) 1701.

[6] M.H. Zainal-Abidin, M. Hayyan, G.C. Ngoh, W.F. Wong, C.Y. Looi, J. Control. Release 316 (2019) 168.
[7] S.N. Pedro, M.G. Freire, C.S.R. Freire, A.J.D. Silvestre, Expert Opin. Drug Deliv. 16 (2019) 497.
[8] T. Jeliński, M. Przybyłek, P. Cysewski, Drug Dev. Ind. Pharm. 45 (2019) 1120.
[9] S. Sut, M. Faggian, V. Baldan, G. Poloniato, I. Castagliuolo, I. Grabnar, B. Perissutti, P. Brun, F. Maggi, D. Voinovich, G. Peron, S. Dall'Acqua, Molecules (Basel, Switzerland) 22 (2017).
[10] K.O. Wikene, E. Bruzell, H.H. Tønnesen, Eur. J. Pharm. Sci. 80 (2015) 26.
[11] K.O. Wikene, E. Bruzell, H.H. Tønnesen, J. Photochem. Photobiol. B 148 (2015) 188.
[12] K.O. Wikene, H.V. Rukke, E. Bruzell, H.H. Tønnesen, J. Photochem. Photobiol. B 171 (2017) 27.
[13] B.-Y. Zhao, P. Xu, F.-X. Yang, H. Wu, M.-H. Zong, W.-Y. Lou, ACS Sustain. Chem. Eng. 3 (2015) 2746.
[14] I.P.E. Macário, H. Oliveira, A.C. Menezes, S.P.M. Ventura, J.L. Pereira, A.M.M. Gonçalves, J.A.P. Coutinho, F.J.M. Gonçalves, Sci. Rep. Lond. (2019) 9.
[15] K. Radošević, M.C. Bubalo, V.G. Srček, D. Grgas, T.L. Dragičević, I.R. Redovniković, Ecotoxicol. Environ. Saf. 112 (2015) 46.
[16] M. Espino, M. Solari, M.D.L.Á. Fernández, J. Boiteux, M.R. Gómez, M.F. Silva, J. Pharm. Biomed. Anal. 167 (2019) 15.
[17] K.G. Grønlien, M.E. Pedersen, H.H. Tønnesen, Int. J. Biol. Macromol. 156 (2020) 394.
[18] J.R. Greene, K.L. Merrett, A.J. Heyert, L.F. Simmons, C.M. Migliori, K.C. Vogt, R.S. Castro, P.D. Phillips, J.L. Baker, G.E. Lindberg, D.T. Fox, R.E. Del Sesto, A.T. Koppisch, PLoS One 14 (2019), e0222211, .
[19] J.N. Pendleton, B.F. Gilmore, Int. J. Antimicrob. Agents 46 (2015) 131.
[20] K.D. Weaver, M.P. Van Vorst, R. Vijayaraghavan, D.R. Macfarlane, G.D. Elliott, Biochim. Biophys. Acta Biomembr. 1828 (2013) 1856.
[21] U. Jacobi, M. Kaiser, R. Toll, S. Mangelsdorf, H. Audring, N. Otberg, W. Sterry, J. Lademann, Skin Res. Technol. 13 (2007) 19.
[22] V.P. Torchilin, V. Weissig, The Practical Approach Series, Oxford University Press, Oxford, 2003.
[23] T. Shimanouchi, H. Ishii, N. Yoshimoto, H. Umakoshi, R. Kuboi, Colloids Surf. B Biointerf. 73 (2009) 156.
[24] S.G. Ingebrigtsen, A. Didriksen, M. Johannessen, N. Škalko-Basnet, A.M. Holsæter, Int. J. Pharm. 526 (2017) 538.
[25] K.O. Wikene, H.V. Rukke, E. Bruzell, H.H. Tønnesen, Eur. J. Pharm. Biopharm. 105 (2016) 75.
[26] D. Shah, F.S. Mjalli, Phys. Chem. Chem. Phys. 16 (2014) 23900.
[27] M.A.C. Gutiérrez, M.A.L. Ferrer, C.R. Mateo, F. del Monte, Langmuir 25 (2009) 5509.
[28] Y. Dai, G.-J. Witkamp, R. Verpoorte, Y.H. Choi, Food Chem. 187 (2015) 14.
[29] Z. Yang, T. Itoh, Y.-M. Koo (Eds.), Application of Ionic Liquids in Biotechnology, Springer International Publishing, Cham 2019, pp. 31–59.
[30] A. Mitar, M. Panić, J. Prlić Kardum, J. Halambek, A. Sander, K. Zagajski Kučan, I. Radojčić Redovniković, K. Radošević, Chem. Biochem. Eng. Q. 33 (2019) 1.
[31] L.K. Savi, M.C.G.C. Dias, D. Carpine, N. Waszczynskyj, R.H. Ribani, C.W.I. Haminiuk, Int. J. Food Sci. Tech. 54 (2019) 898.
[32] M. Rasouli, Clin. Biochem. 49 (2016) 936.
[33] H.-G. Meland, A. Røv-Johnsen, G. Smistad, M. Hiorth, Colloids Surf. B Biointerf. 114 (2014) 45.
[34] M.R. Moncelli, L. Becucci, R. Guidelli, Biophys. J. 66 (1994) 1969.
[35] A.D. Petelska, Z.A. Figaszewski, Biophys. J. 78 (2000) 812.
[36] Y. Zhou, R.M. Raphael, Biophys. J. 92 (2007) 2451.
[37] M. Guiral, C. Neitzel, M.S. Castell, N. Martinez, M. Giudici-Orticoni, J. Peters, Eur. Phys. J. E (2018) 8.
[38] S. Honary, F. Zahir, Trop. J. Pharm. Res. 12 (2013).
[39] J. Sabın, G. Prieto, J.M. Ruso, R. Hidalgo-Álvarez, F. Sarmiento, Eur Phys J E 20 (2006) 401.
[40] A.V. Yadav, M.S. Murthy, S.A. Somanath, S. Sakhare, Ind. J. Pharm. Edu. Res. 45 (2011) 402.
[41] T.M. Allen, L.G. Cleland, Biochim. Biophys. Acta Biomembr. 597 (1980) 418.
[42] D. Papahadjopoulos, K. Jacobson, S. Nir, T. Isac, Biochim. Biophys. Acta Biomembr. 311 (1973) 330.
[43] M. Rappolt, G. Rapp, Eur. Biophys. J. 24 (1996) 381.
[44] L.M. Crowe, J.H. Crowe, Biochim. Biophys. Acta Biomembr. 1064 (1991) 267.
[45] J. Drazenovic, H. Wang, K. Roth, J. Zhang, S. Ahmed, Y. Chen, G. Bothun, S.L. Wunder, BBA - Biomembranes 1848 (2015) 532.
[46] M.I. Morandi, M. Sommer, M. Kluzek, F. Thalmann, A.P. Schroder, C.M. Marques, Biophys. J. 114 (2018) 2165.
[47] U. Baxa, Methods Mol. Biol. 1682 (2018) 73.
[48] O. Et-Thakafy, N. Delorme, C.D. Gaillard, C. Mériadec, F. Artzner, C. Lopez, F. Guyomarc'h, Langmuir 33 (2017) 5117.
[49] D.K. Shah, S. Khandavilli, R. Panchagnula, Methods Find. Exp. Clin. Pharmacol. 30 (2008) 499.
[50] R.R. Warner, K.J. Stone, Y.L. Boissy, J. Invest Dermatol. 120 (2003) 275.
[51] R. Mendelsohn, C.R. Flach, D.J. Moore, Biochim. Biophys. Acta 1758 (2006) 923.
[52] A. Banerjee, K. Ibsen, Y. Iwao, M. Zakrewsky, S. Mitragotri, Adv. Healthc. Mater. 6 (2017) 1601411.
[53] S. Olsztyńska-Janus, A. Pietruszka, Z. Kiełbowicz, M.A. Czarnecki, Spectrochim. Acta A Mol. Biomol. Spectrosc. 188 (2018) 37.
[54] J. Covi-Schwarz, V. Klang, C. Valenta, in: N. Dragicevic, H.I. Maibach (Eds.), Percutaneous Penetration Enhancers Drug Penetration Into/Through the Skin: Methodology and General Considerations, Springer Berlin Heidelberg, Berlin, Heidelberg 2017, pp. 247–254.
[55] T.H. Prasch, G. Knübel, K. Schmidt-Fonk, S. Ortanderl, S. Nieveler, T.H. Förster, Int. J. Cosmet. Sci. 22 (2000) 371.
[56] W. He, X. Guo, L. Xiao, M. Feng, Int. J. Pharm. 382 (2009) 234.
[57] M. Gloor, G. Hirsch, U. Willebrandt, Arch. Dermatol. Res. 271 (1981) 305.
[58] A. Gómez, A. Biswas, C. Tadini, R. Furtado, C. Alves, H. Cheng, J. Braz. Chem. Soc. 30 (2019).
[59] A. Barth, Biochim. Biophys. Acta Bioenerg. 1767 (2007) 1073.
[60] J.-M. Andanson, J. Hadgraft, S.G. Kazarian, J. Biomed. Opt. 14 (2009) 34011.
[61] H. Barańska, J. Kuduk-Jaworska, R. Szostak, A. Romaniewska, J. Raman Spectrosc. 34 (2003) 68.
[62] M. Machado, J. Hadgraft, M.E. Lane, Int. J. Cosmet. Sci. 32 (2010) 397.